第 34 卷第 7 期
2018 年 7 月

无 机 化 学 学 报
CHINESE JOURNAL OF INORGANIC CHEMISTRY

Vol.34 No.7
1365-1372

基于双苯并咪唑及二羧酸配体配合物的合成、结构及抗菌活性

梁丽丽　刘从森　宗智慧　张曼丽　张冰源
曹　睿　王子豪　庞苗苗　李玉杰　陶兆林*
(蚌埠医学院,蚌埠　233030)

摘要：利用双苯并咪唑基配体 4,4′-二(苯并咪唑-1-甲基)联苯(bbmb)与 V 形二羧酸配体 4,4′-二羧苯基醚(H_2dcpe)合成了配合物 $\{[Ni(bbmb)(dcpe)(H_2O)]\cdot 2H_2O\}_n$ (**1**)和 $\{[Mn_2(bbmb)(dcpe)_2(H_2O)]\cdot 1.5H_2O\}_n$ (**2**)。通过红外、元素分析、X 射线单晶衍射、热重分析等检测手段对配合物结构进行了表征。配合物 **1** 是具有 *sql* 拓扑构型的二维层状化合物。配合物 **2** 呈现出含有四核锰构型的二维层状结构。体外抗菌实验证明 2 个配合物都表现出良好的抗菌活性。

关键词：苯并咪唑配体；晶体结构；抗菌活性；配合物
中图分类号：O614.71+1；O614.81+3　　**文献标识码**：A　　**文章编号**：1001-4861(2018)07-1365-08
DOI：10.11862/CJIC.2018.163

Syntheses, Crystal Structures and Antimicrobial Activities of Two Coordination Polymers Based on Bisbenzimidazole Ligands and V-Shaped Dicarboxylates

LIANG Li-Li　LIU Cong-Sen　ZONG Zhi-Hui　ZHANG Man-Li　ZHANG Bing-Yuan
CAO Rui　WANG Zi-Hao　PANG Miao-Miao　LI Yu-Jie　TAO Zhao-Lin*
(*Bengbu Medical College*, *Bengbu*, *Anhui* 233030, *China*)

Abstract: Two coordination polymers $\{[Ni(bbmb)(dcpe)(H_2O)]\cdot 2H_2O\}_n$ (**1**) and $\{[Mn_2(bbmb)(dcpe)_2(H_2O)]\cdot 1.5H_2O\}_n$ (**2**) have been synthesized utilizing a linear benzimidazole ligand 4,4′-bis (benzimidazol-1-ylmethy1)biphenyl) (bbmb) combined with a V-shaped dicarboxylates ligand 4,4′-dicarboxydiphenyl ether (H_2dcpe). Compound **1** possesses a 2D thick layer structure with *sql* topology. Compound **2** possesses a 2D thick layer network with a linear tetranuclear Mn_4 cluster within the network. The *in vitro* antimicrobial activities showed that both compounds have effective inhibiting effects. CCDC: 1525542, **1**; 1525543, **2**.

Keywords: benzimidazole ligand; crystal structure; antimicrobial properties; coordination polymers

0 Introduction

With the increase of drug-resistant microbial strains, searching for new antibacterial and antifungal chemotherapeutics is becoming a formidable task for pharmaceutists and medicinal chemists. Since imidazoles are biocompatible and antimicrobial, many medicinal applications have been found. The imidazole derivatives are one of the important families in heterocyclic compounds, and many of them have recently been used in medicine and pesticide fields[1-3]. The design and assembly of benzimidazole compounds have attracted great attention for their antifungal, antibacterial, antimicrobial, antiparasitic, antiviral and antitumor activities[4-10]. Extensive efforts to develop new antibacterial metal-based benzimidazole compounds

收稿日期：2018-02-14。收修改稿日期：2018-03-30。
安徽省高校自然科学研究重点项目(No.KJ2017A242,KJ2016A471)和蚌埠医学院科技发展基金项目(No.BYKY17121)资助。
*通信联系人。E-mail：tao6838@163.com；会员登记号：S06N3381M1508。

have been observed[11-16]. Benzimidazole-1-ly-based ligands are also good candidates of N-donor linkers to construct coordination polymers of different configurations[17-18]. Herein, we employed a linear benzimidazole-1-ly-based ligand 4,4′-bis(benzimidazol-1-ylmethy1) biphenyl) (bbmb) combined with a V-shaped dicarboxylates ligand 4,4′-dicarboxydiphenyl ether (H_2dcpe), and successfully synthesized two coordination polymers with different layer structures.

1 Experimental

1.1 Materials and instruments

The ligand bbmb 4,4′-bis(benzimidazole-1-ylmethyl)biphenyl (bbmb) was synthesized according to the reported method with a little modification[19]. All other starting materials were commercially purchased and used as received. IR spectra were performed from KBr pellets in the range of 4 000~400 cm^{-1} with a NICOLET iS50 spectrometer. C, H and N elemental analyses were carried out with an Elementar Vario-EL CHNS elemental analyzer. Solid-state UV-Vis diffuse reflectance spectra were obtained at room temperature on finely ground samples with Shimadzu UV-3600 double monochromator spectrophotometer using barium sulfate ($BaSO_4$) as a 100% reflectance standard. Powder X-ray diffraction (XRD) intensities was measured on a Bruker D8 ADVANCE X-Ray Diffractometer (Cu $K\alpha$, λ=0.154 056 nm) in the 2θ range of 5°~50° in which the X-ray tube was operated at 40 kV and 40 mA. Thermogravimetrical (TG) analyses were performed from 25 to 700 ℃ at a heating rate of 10 ℃·min^{-1}, under N_2 atmosphere with a flow rate of 50 mL·min^{-1} on a simultaneous STA 449-F5 thermal analyzer.

1.2 Synthesis of {[Ni(bbmb)(dcpe)(H_2O)]·2H_2O}$_n$ (1)

A mixture of bbmb (21 mg, 0.05 mmol), H_2dcpe (13 mg, 0.05 mmol) and $Ni(NO_3)_2·6H_2O$ (29 mg, 0.1 mmol) in 4 mL mixed solvent of DMF/H_2O (1:3, *V*/*V*) was placed in a 25 mL Teflon-lined stainless steel container and heated to 100 ℃ for 48 h. The reaction system was cooled to room temperature. Green block crystals of **1** were collected by filtration and dried in air (Yield: 48% based on bbmb). Anal. Calcd. for $C_{42}H_{35}N_4NiO_8$(%): C 64.47, H 4.51, N 7.16; Found(%): C 64.41, H 4.54, N 7.12. IR: (KBr pellet, cm^{-1}): 3 742 (w), 3 423(s), 2 926(w), 2 363(w), 1 598(m), 1 548(m), 1508(w), 1 386(s), 1 240(w), 1 160(s), 1 116(w), 876 (w), 792(w), 744(w), 658(w), 499(w), 419(w).

1.3 Synthesis of {[Mn_2(bbmb)(dcpe)$_2$(H_2O)]·1.5H_2O}$_n$ (2)

A mixture of bbmb (21 mg, 0.05 mmol), H_2dcpe (13 mg, 0.05 mmol) and $Mn(NO_3)_2$ (50% aq. 0.1 mmol) in 4 mL mixed solvent of DMF/H_2O (2:2, *V*/*V*) was placed in a 25 mL Teflon-lined stainless steel container and heated to 110 ℃ for 48 h. Then the reaction system was cooled to room temperature slowly. Colorless block crystals of **2** were collected by filtration and dried in air (Yield: 61% based on H_2dcpe). Anal. Calcd. for $C_{56}H_{43}Mn_2N_4O_{12.5}$(%): C 62.17, H 4.01, N 5.18; Found(%): C 62.12, H 4.05, N 5.13. IR: (KBr pellet, cm^{-1}): 3 428(m), 3 099(w), 2 926(w), 1 667(w), 1 600 (s), 1 554 (m), 1 502 (s), 1 397 (s), 1 334(m), 1 242(s), 1 155(m), 1 010(w), 872(m), 792(m), 742(m), 702(m), 630(w), 513(w).

1.4 Crystallography

Single crystals with suitable dimensions for **1** and **2** were selected for single crystal X-ray diffraction measurements and the data were collected at 296(2) K on a Bruker Apex Smart APEX Ⅱ X-ray Single Crystal diffractometer. Data reductions and absorption corrections were performed using the SAINT and SADABS[21a] software packages, respectively. The structure was solved by direct methods and refined by full matrix least-squares methods on F^2 using the SHELXS-97 and SHELXL-97 programs[21b]. The coordinates of the nonhydrogen atoms were refined anisotropically, and the positions of the H-atoms were generated geometrically. There are some highly disordered guest solvent molecules, which could hardly be located in the X-ray structure because of severe thermal disorder. The SQUEEZE subroutine of the PLATON software suit was used to remove the scattering from the highly disordered guest molecules[22]. The resulting new files were used to further refine the structures. The numbers of guest molecules in **1** and **2** were obtained by considering the number of electrons filtered by

SQUEEZE combining with elemental analyses and TGA data. The result data reveal that **1** contains two H_2O molecules, and **2** contains one and a half H_2O molecules. Basic information pertaining to crystal parameters and structure refinement is summarized in Table 1.

CCDC: 1525542, **1**; 1525543, **2**.

Table 1　Crystal data and structure refinements for 1 and 2

	1	2
Formula	$C_{42}H_{31}N_4NiO_6$	$C_{56}H_{40}Mn_2N_4O_{11}$
Formula weight	746.42	1 054.80
Crystal system	Triclinic	Monoclinic
Space group	$P\bar{1}$	$C2/c$
a / nm	1.323 3(4)	3.253 7(8)
b / nm	1.329 2(4)	1.100 1(3)
c / nm	1.368 1(4)	2.905 3(7)
α / (°)	96.467(5)	
β / (°)	111.970(4)	109.648(4)
γ / (°)	114.294(4)	
V / nm^3	1.930 3(9)	9.793(4)
Z	2	8
D_c / (g·cm^{-3})	1.284	1.431
F(000)	774	4 336
Crystal size / mm	0.28×0.24×0.22	0.28×0.24×0.22
μ / mm^{-1}	0.554	0.584
Total reflection	6 601	8 604
Unique reflection	4 444	5 378
R_{int}	0.043 6	0.080 4
GOF on F^2	1.071	0.994
R_1, wR_2 [$I>2\sigma(I)$]	0.050 6, 0.112 9	0.055 7, 0.152 8
R_1, wR_2 (all data)	0.080 2, 0.122 1	0.088 1, 0.173 5

1.5　Biological activity test

The antimicrobial activities of **1**, **2** and bbmb ligand were determined *in vitro* using agar well diffusion method[20]. Growth inhibitory activity against *S. aureus* (MTCC 3160), *E. coli* (MTCC 51), *dysentery bacillus*, *C. albicans* and *P. aeruginosa* were measured. The bacterial strains grown on nutrient agar at 37 ℃ for 18 h were suspended in saline solution (0.85% NaCl) and adjusted to a turbidity of 0.5 MacFarland standards. The suspension was used to inoculate sterile Petri plates of 9.0 cm diameter in which the test compounds were grown. Compounds **1**, **2** and bbmb ligand were dissolved in dimethylsulfoxide (DMSO) to prepare three different concentrations for evaluation of dose response. Antibacterial activities of the compounds were evaluated by measuring the inhibition zone diameters (IZD).

2　Results and discussion

2.1　Crystal structures

Compound **1** crystallizes in the triclinic space group $P\bar{1}$. The asymmetric unit consists of one Ni atom, two half bbmb ligands, one dcpe ligand and one coordinated water molecule. The Ni atom has an octahedral coordination sphere, which consists of four oxygen atoms (Ni-O 0.202 0(2)~0.219 9(2) nm) from two dcpe molecules and one water molecule, two nitrogen atoms (Ni-N 0.205 nm) from two bbmb molecules (Fig.1). The two benzene rings of the dcpe ligand are crossed with a dihedral angle of 124.7°. The dcpe ligands connect Ni atoms through two carboxylates alternately to form wine chains (Fig.2, black

color). The wine chains are further connected by two kinds of bbmb ligands. Two bbmb ligands connect Ni atoms to form a helical chain. The bbmb ligands have similar configurations. The two center benzene rings of bbmb ligands are coplanar. The two benzimidazole rings of one bbmb ligand are parallel to each other, located on the opposite side of the two center benzene rings. There are π-π interactions between the benzimidazole rings of bbmb ligands. The two benzimidazole rings of one bbmb ligand are parallel to benzimidazole rings of other two bbmb ligands. The dihedral angle is 0° and the plane-to-plane distance is 0.334 and 0.362 nm, respectively[23] (Fig.2). So the bbmb ligands are further connected through two kinds of π-π interactions. Each Ni atom is connected to two bbmb ligands and two dcpe ligands. Topologically, dcpe and bbmb ligands can be simplified into chains of different lengths and Ni atoms as four-connected nodes. The whole structure can be reduced to a 4-noded uninodal network. Analysis with Topos 4.0 software, the whole framework can be classified as *sql* topology with the Schlfli symbol of $\{4^4 \cdot 6^2\}$. The wine chains formed by dcpe ligands and the helical chains formed by bbmb ligands are interwoven together by sharing Ni atoms and extended indefinitely (Fig.3a). The whole framework is extended indefinitely along two

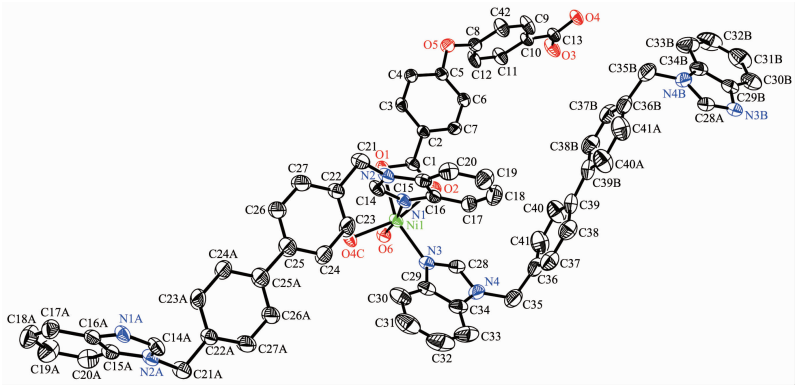

Displacement ellipsoids are drawn at the 30% probability level; H atoms are omitted for clarity; Symmetry codes: A: 3–*x*, 2–*y*, 2–*z*; B: –1+*x*, –1+*y*, –1+*z*; C: 1+*x*, 1+*y*, 1+*z*

Fig.1 Coordination environment of Ni atom showing the atom numbering scheme

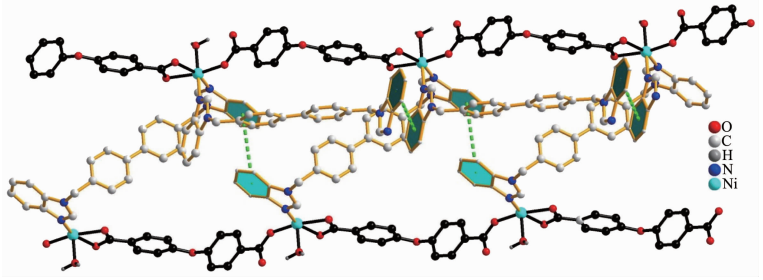

Dotted lines: π-π interactions between the benzimidazole rings of bbmb ligand

Fig.2 Wine chains (black color) formed by dcpe ligands connecting Ni atoms and further connected by two kinds of bbmb ligands

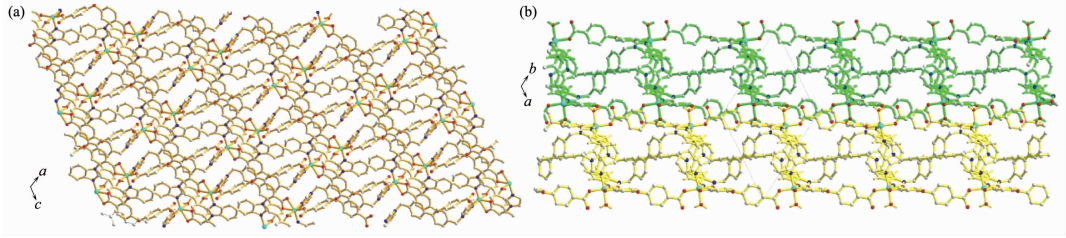

Fig.3 (a) Extended 2D framework of **1** viewed along the *b* axis; (b) Two disconnected thick layer networks described in different colors

directions to form a 2D thick layer structure (Fig.3b).

Compound **2** crystallizes in the monoclinic space group *C*2/*c*. The asymmetric unit consists of two crystallographically unique Mn atoms, one bbmb ligand, two dcpe ligands and one coordinated water molecule (Fig.4). Mn1 and Mn2 atoms are both in an octahedral structure, coordinated by five oxygen atoms from two dcpe ligands and one water molecule (Mn-O 0.210 4(3) ~0.238 4(3) nm), one nitrogen atom from bbmb ligand (Mn-N 0.221 7(3), 0.222 7(4) nm). Mn1 and Mn2 atoms are bridged by two carboxylate groups in μ_2-η^1:η^1 fashion and a μ_2-O_{water}. Mn2 and Mn2 atoms are bridged by two μ_2-$O_{carboxyl}$ to form a rhombus structure with Mn2 ⋯Mn2 separations of 0.357 3(1) nm. So Mn1-Mn2-Mn2-Mn1 is bridged together to afford a linear tetranuclear Mn_4 cluster. The Mn_4 cluster is connected by ten dcpe ligands and four bbmb ligands (Fig.5a). The linear tetranuclear clusters are further connected through carboxylates to form a linear chain, which is further connected by dcpe ligands to form an infinite 2D network (Fig.5b). The biphenyl rings of the bbmb ligand are not coplanar with the dihedral angle of

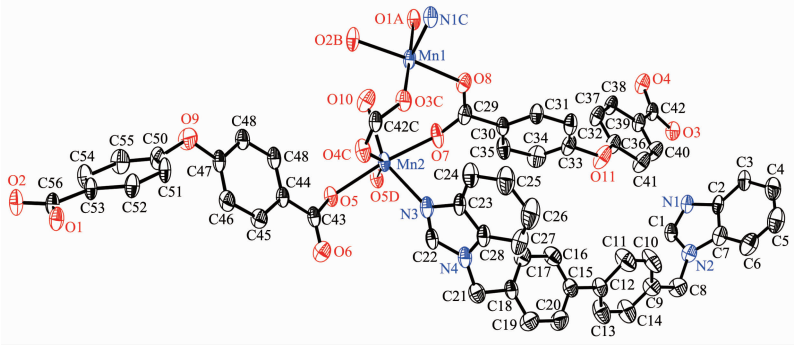

Displacement ellipsoids are drawn at the 30% probability level; H atoms are omitted for clarity;
Symmetry codes: A: *x*, 1−*y*, 05+*z*; B: 0.5−*x*, 0.5+*y*, 0.5−*z*; C: *x*, 1−*y*, −05+*z*; D: 0.5−*x*, 0.5−*y*, 1−*z*

Fig.4　Coordination environments of Mn1 and Mn2

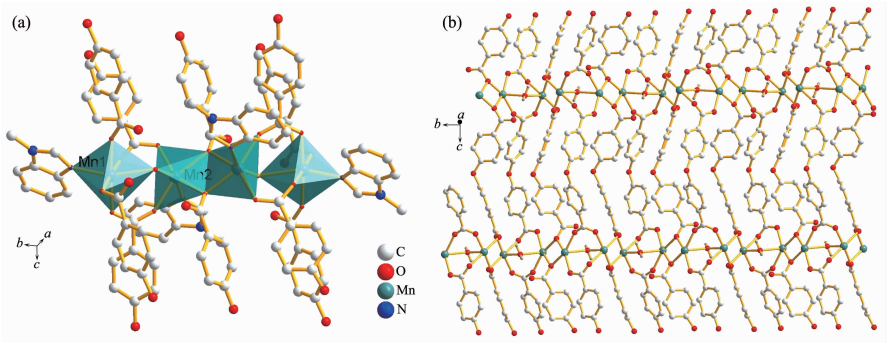

Fig.5　(a) Coordination environment of the linear Mn_4 cluster; (b) Linear Mn_4 clusters further connected through carboxylate to form a linear chain

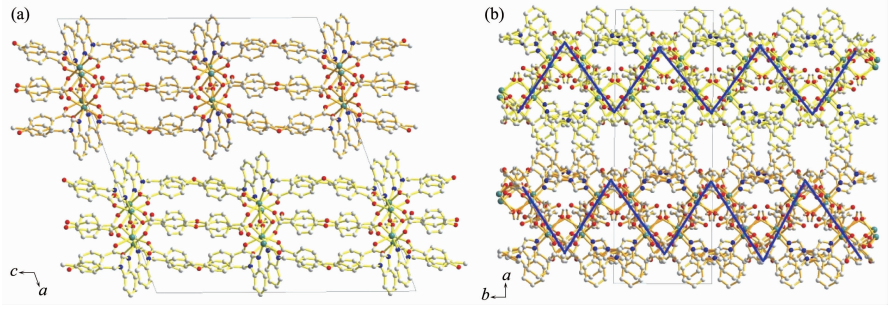

Two thick layer networks described with different colors in (b)

Fig.6　(a) Two disconnected 2D layer networks; (b) Zigzag chains inside the layer networks viewed along the *c* axis

42.5(2)°. The two benzimidazole rings are in the same side of the biphenyl rings connecting Mn1 and Mn2 atoms, respectively. The linear tetranuclear chains of the 2D network are further connected by bbmb ligands in another direction to increase the thickness of the layer network. Fig.6a shows two disconnected 2D layer networks differentiated with different colors. The Mn_4 clusters chains are zigzag-shaped inside the network viewed along the *c* axis (Fig.6b).

2.2 XRD and thermogravimetric analyses

Powder X-ray diffraction (XRD) experiments were carried out for the two compounds to confirm the phase purities of the bulk materials. The experimental and structure-simulated XRD patterns of the two compounds are compared (Fig.7). The main peaks of the bulk synthesized materials and the simulated match well, indicating the purities of the two compounds. To estimate the stability of the coordination architecture, the thermal behaviors of the two compounds were investigated on crystalline samples by thermal gravimetric analysis (TGA). The TGA curves (Fig.8) show compound **1** is thermally stable up to *ca.* 385 ℃. The weight loss of 9.3% at about 140 ℃ should be attributed to the loss of two guest H_2O molecules (Calcd. 4.6%) and adsorbed H_2O molecules. An abrupt weight loss at about 385 ℃ should be due to the pyrolysis of the main structure. For compound **2**, the gradual weight loss of 5.0% at 230 ℃ should be attributed to the loss of 1.5 guest H_2O molecules (Calcd. 2.5%). Decomposition of the framework occurred at 385 ℃, indicating that the main framework collapsed at a relatively high temperature under a nitrogen atmosphere.

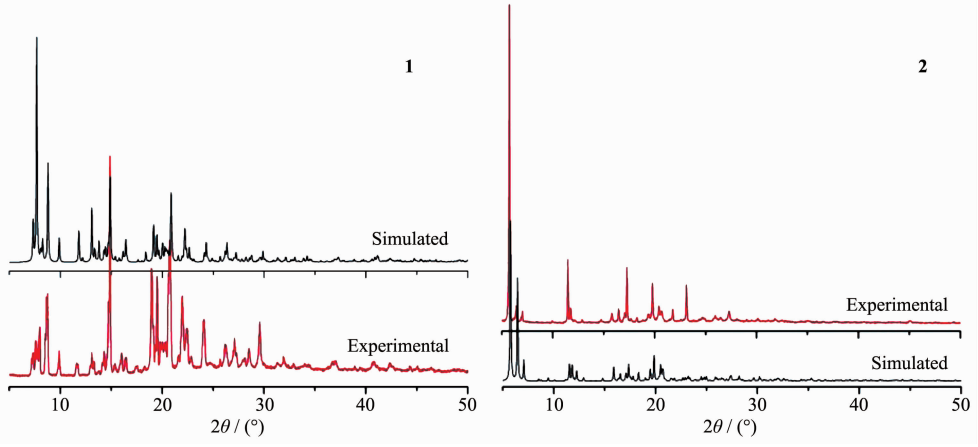

Fig.7 Powder X-ray diffraction patterns of **1** and **2**

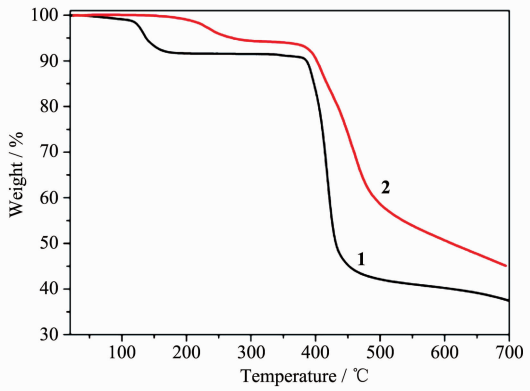

Fig.8 TG curves of **1** and **2**

2.3 Solid UV-Vis absorbance spectra

The solid-state UV-Vis absorbance spectra of free bbmb, H_2dcpe and compound **1** were measured at room temperature. Compound **1** exhibits three absorbance bands in the range of 200~850 nm (Fig.9).

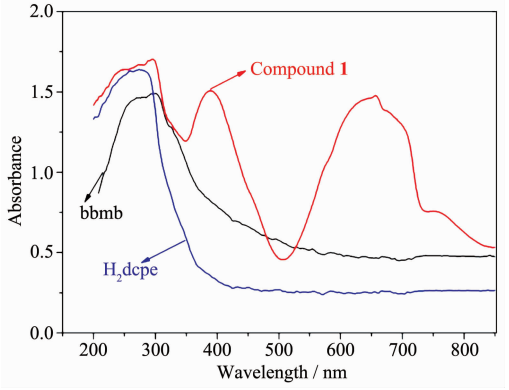

Fig.9 Solid-state UV-Vis absorbance spectra of bbmb, H_2dcps and compound **1**

The absorbance bands at 200~350 nm, similar with that of bbmb, a little red shift to that of H_2dcpe, can be assigned to $\pi \rightarrow \pi^*$ transitions of the phenyl ring ligands. The absorbance bands at about 400 nm and the broad bands at 600~700 nm of **1**, can be attributed to $[^3T_{1g}(p) \rightarrow {}^3A_{2g}]$ and $[^3T_{1g}(F) \rightarrow {}^3A_{2g}]$ transitions of Ni(Ⅱ) compounds[24-26].

2.4 Antimicrobial activities

The antimicrobial activities of **1**, **2** and bbmb ligand (DMSO solution) were tested with different bacteria using diffusion method. The diameters of the antibacterial rings were tested to evaluate the antimicrobial activities and the results were listed in Table 2. The results showed that compound **1** exhibited obviously fungicidal activity against *S. aureus* and *E. coli*. Compound **2** showed significant inhibitory effect on *C. albicans*, *S. aureus*, *E. coli* and *dysentery bacillus*. The bbmb ligand only showed very little inhibiting effect on *dysentery bacillus*, and no inhibitory effect on other bacteria. From the *in vitro* antibacterial assay, it is observed that compound **1** possesses exclusive inhibitory activities, while compound **2** shows extensive antibacterial effect. The coordination compounds showed enhanced antimicrobial activity in many cases over the free bbmb ligand. The results could be explained on the basis of chelation theory and the presence of suitable metal ions is essential for microbiological activity of the coordination polymer[27]. Compound **2** has greater potential medical value worthy of further investigation.

Table 2　Antibacterial activities of bbmb ligand and compounds 1 and 2

Compound	Dose / (mg·mL^{-1})	*C. albicans*	*S. aureus*	*E. coli*	*dysentery bacillus*	*P. aeruginosa*
bbmb	0.7	×	×	×	√	×
1	0.5	×	√	√	×	×
2	0.3	√	√	√	√	×

3　Conclusions

Two coordination polymers were synthesized by hydrothermal methods with the benzimidazole ligand combined with a V-shaped dicarboxylates ligand. Both compounds possess unique 2D thick layer network. Compound **1** exhibits a rare layered 4-connected structure with *sql* topology. The biological activity test indicated that compound **2** showed enhanced antimicrobial activity to *C. albicans*, *S. aureus*, *E. coli* and *dysentery bacillus* compared to bbmb ligand. The coordination polymers were found to display considerable antimicrobial activity.

References:

[1] Horton D A, Bourne G T, Smythe M L. *Chem. Rev.*, **2003**, **103**:893-930

[2] Shalini K, Sharma P K, Kumar N. *Der Chemica Sinica*, **2010**, **1**:36-47

[3] Kim E, Yang J, Kim H O, et al. *Biomaterials*, **2013**,**34**:4327-4338

[4] CHEN Qing(陈青), LU Li-Ping(卢丽萍). *Chinese J. Inorg. Chem.*(无机化学学报), **2016**,**32**(6):1001-1008

[5] Fang X J, Jeyakkumar P, Avula S R, et al. *Bioorg. Med. Chem. Lett.*, **2016**,**26**:2584-2588

[6] Zhang J, Yao D, Jiang Y. *Bioorg. Chem.*, **2017**,**72**:168-181

[7] Anderson E B, Long T E. *Polymer*, **2010**,**51**:2447-2454

[8] Özdena S, Atabey D, Yıldız S, et al. *Bioorg. Med. Chem.*, **2005**,**13**:1587-1597

[9] Poyraz M, Sari M, Demirci F, et al. *Polyhedron*, **2008**,**27**:2091-2096

[10]ZHANG Qi-Long(张奇龙), FENG Guang-Wei(冯广伟), WANG Li(王丽), et al. *Chinese J. Inorg. Chem.*(无机化学学报), **2014**,**30**(5):1025-1030

[11]McCann M, Curran R, Ben-Shoshan M, et al. *Dalton Trans.*, **2012**,**41**:6516-6527

[12]Arjmand F, Mohani B, Ahmad S. *Eur. J. Med. Chem.*, **2005**, **40**:1103-1110

[13]ZHAO Hai-Yan(赵海燕), YANG Xiao-Dong(杨晓东), LI Na(李娜). *Chinese J. Inorg. Chem.*(无机化学学报), **2017**,**33**(4):685-691

[14]Aghatabay N M, Neshat A, Karabiyik T, et al. *Eur. J. Med. Chem.*, **2007**,**42**:205-213

[15]Ou Z B, Lu Y H, Lu Y M, et al. *J. Coord. Chem.*, **2013**,**66**:2152-2165

[16]Kalinowska-Lis U, Felczak A, Chcińska L, et al. *J. Organomet. Chem.*, **2014**,**749**:394-399

[17]Feng R, Hou Y, Wu Z Z, et al. *Z. Anorg. Allg. Chem.*, **2015**,**641**:1918-1925

[18]Liang L, Xue H, Chen F, et al. *J. Mol. Struct.*, **2017**,**1148**: 247-253

[19]Dobrzańska L, Lloyd G O, Jacobs T, et al. *J. Mol. Struct.*, **2006**,**796**:107-113

[20]Singh K, Barwa M S, Tyagi P. *Eur. J. Med. Chem.*, **2007**,**42**: 394-402

[21](a)Sheldrick G M. *SADABS*, University of Göttingen, Germany, **1996**.

(b)Sheldrick G M. *SHELX*-97, *Program for the Solution and the Refinement of Crystal Structures*, University of Göttingen, Germany, **1997**.

[22]Spek A L. *J. Appl. Cryst.*, **2003**,**36**:7-13

[23]Janiak C. *J. Chem. Soc. Dalton Trans.*, **2000**,**29**:3885-3896

[24]Yam V V W, Lo K K W. *Chem. Soc. Rev.*, **1999**,**28**:323-334

[25]Sarma D, Ramanujachary K V, Lofland S E, et al. *Inorg. Chem.*, **2009**,**48**:11660-11676

[26]Qin L, Hu J, Li Y, et al. *Cryst. Growth Des.*, **2012**,**12**:403-413

[27]Mahmoud W H, Mohamed G G, El-Dessouky M M I. *Spectrochim. Acta Part A*, **2014**,**122**:598-608